# Finite Element Analysis for Molar-Tooth Under Different loading conditions

## تحليل الإجهادات فى الضرس تحت حالات تحميل مختلفة باستخدام طريقة العناصر المحددة

**Hamza A. Ghulman, and Mohammed W. Al-Hazmi**
**Mechanical Engineering Department,**
**Umm Al-Qura University**
**P.O. Box 5555**
**Makkah, Kingdom of Saudi Arabia**
**Phone: +966 (2) 52700920- Ext. 2590**
**Fax: +966 (2) 5270027**
**Email: hghulman@uqu.edu.sa and malhazmi@uqu.edu.sa**

الملخص: يواجهة الضرس حالات تحميل مختلفة وإجهادات فى أجواء مختلفة من درجات الحرارة، وتكون حالات التحميل هذه من العوامل الرئيسية فى ضعف التركيب البنائى للضرس. بالاضافة الى ذلك، هذه الأحمال المتكررة ستولد إنهيار الضرس نتيجة الإعياء. لذلك هدف هذه الدراسة هو أن نتحرى تحليل الاجهادات والتشوهات للضرس باستخدام طريقة العناصر المحددة. وتحقيق هذه الدراسة باستخدام برنامج العناصر المحددة (ANSYS). علاوة على ذلك، النتائج الموجودة فى هذه الدراسة لتحليل الإجهاد فى الضرس تحت تأثير أحمال بزوايا مختلفة، ويشير إلى أن أقصى إجهاد للقص والتشوة يزيد بنقص زاوية تأثير الحمل.

**Abstract:** The molar tooth faces different loading conditions and stresses under environments of different temperatures, these loading conditions produces a major factors in weakness of the tooth structure. In addition, this cyclic loads will generate a fatigue failure for the tooth. So that, The objective of this study is to investigate of the stresses and deformations analysis for molar tooth using finite elements method. The study investigation is completed and achieved by using Finite Element package ANSYS. Furthermore, The results are illustrated in this study to investigate the stress analysis of the molar tooth under loading conditions with different angles, and indicate that the maximum shearing stress and deformation is increased with decreasing directional angle of the applied load.

Accepted December 31, 2008

## 1 Introduction:

The marginal ridges of posterior teeth are considered to be of primary importance in providing structural strength to the crown. The crown of the tooth is considered to behave as a structural laminate, and breaking the continuity of enamel layer significantly reduces tooth rigidity by *Tidmarsh (1976)*. The marginal ridge has a greater thickness of enamel than other areas, so that the loss of tooth structure in this area associated with restorative procedures may be a major factor in weakening teeth by *Eshleman et al, (1988)*. Loss of one or both marginal ridges weakens the tooth and makes it more susceptible to fracture. Mechanical stress has also been implicated in caries initiation (including smooth surface caries), so that stress distribution in proximal enamel is also relevant to this debate [*Hansen et al, (1990), Mondelli et al, (1980), Morin et al, (1988)*, and *Reeh et al, (1989)*].

The stresses generated in marginal ridges and proximal enamel during normal occlusal function, and changes in stress patterns following loss of one or both marginal ridges, have not been widely investigated. Despite numerous finite element analysis (FEA) studies of occlusal loads on teeth, surprisingly little is known of patterns of stress and strain in marginal ridges or proximal enamel [*Darendeliler et al, (1992), Goel et al, (1990), Kaewsuriyathumrong et al, (1993), Thresher et al, (1973)*, and *Arola et al, (2001)*]. Since finite element models involve a number of assumptions, theoretical models require validation before the results can be reliably interpreted. The use of FEA combined with experimental strain measurement should yield information that is more directly applicable to the clinical situation. However, few of the above studies have included strain gauge measurements, despite their widespread use with extracted teeth, [*Sakaguchi et al, (1991), Roberto et al, (2004), and Ausiello et al, (2001)*].

## 2 Background of molar tooth using FEA analysis:

There is several studies for tooth analysis using FE method such as *Genovese, et al, (2004)* investigate the mechanical behavior of a new customized post system built up with a composite framework presently utilized for crowns, bridges, veneers and inlay/onlay dental restorations. The material has been shaped so to follow perfectly the profile of the root canal in order to take advantage of the better mechanical properties of composites with respect to metallic alloys commonly used for cast posts. The analysis has been carried out with 3-D finite element models previously validated on the basis of experimental work. The new post system has been compared to a variety of restorations using either prefabricated or cast posts. The structural efficiency of the new restoration has been evaluated for an upper incisor under different loading conditions (mastication, bruxism, impact).

Results prove that maximum stress values in restored teeth are rather insensitive to post types and materials. However, the new customized composite restoration allows to reduce significantly the stresses inside the dentinal regions where conservative clinical interventions are not possible [*Genovese et al, (2004)*].

*Pattijn, et al,* (2005) evaluate the modal behaviour of the bone-implant-transducer (Osstell) system by means of finite element analyses. The influence of different parameters was determined: (1) the type of implant anchorage being trabecular, cortical, uni-cortical, or bi-cortical, (2) the implant diameter, (3) the length of the implant embedded in the bone, and (4) the bone stiffness.

The type of anchorage determines the resulting modal behaviour of the implant–transducer system. A rigid body behaviour was found for a uni-cortical anchoring and for a homogeneous anchoring with low bone stiffness (≤1000 MPa), whereas a bending behaviour was found for a homogeneous anchoring with a high bone stiffness (≥5000 MPa) and for a bi-cortical anchorage. The implant dimensions influence the values for the resonance frequencies. Generally, an increase in implant diameter or implant length (in bone) results in higher resonance frequencies. This study also showed that resonance frequencies in case of rigid body behaviour of the implant–transducer system are more sensitive to changes in bone stiffness than resonance frequencies in case of bending behaviour. In conclusion, it seems that the Osstell transducer is suited for the follow-up in time of the stability of an implant, but not for the quantitative comparison of the stability of implants [*Pattijn et al*, (2005)].

*DeHoff, et al*, (2004) studied the viscoelastic option of the ANSYS finite element program to calculate residual stresses in an all-ceramic FPD for four ceramic–ceramic combinations. A three-dimensional finite element model of the FPD was constructed from digitized scanning data and calculations were performed for four systems: (1) IPS Empresss 2, a glass-veneering material, and Empresss 2 core ceramic; (2) IPS ErisTM a low fusing fluorapatite-containing glass-veneering ceramic, and Empresss 2 core ceramic; (3) IPS Empresss 2 veneer and an experimental lithium-disilicate-based core ceramic; and (4) IPS ErisTM and an experimental lithium–disilicate-based core ceramic. The maximum residual tensile stresses in the veneer layer for these combinations are as follows: (1) 77MPa, (2) 108MPa, (3) 79 MPa, and (4) 100MPa. These stresses are relatively high compared to the flexural strengths of these materials. In all cases, the maximum residual tensile stresses in the core frameworks were well below the flexural strengths of these materials. We conclude that the high residual tensile stresses in all-ceramic FPDs with a layering ceramic may place these systems in jeopardy of failure under occlusal loading in the oral cavity [*Paul, et al*, (2004)].

*Ueda, et al*, (2004). Invest I sate the comparison of photoelastic analysis, the stress distribution in a fixed prosthesis with 3 parallel implants, to the stress distribution in the same prosthesis in the existence of an angled central implant. Two photoelastic resin models were made and a polariscope was used in the visualization of isochromatic fringes formed in the models when axial loads of 2 kg, 5 kg and 10 kg were applied to a unique central point of the prosthesis. The presence of inducted tensions (preloads) was observed in the models after applying torque to the retention screws. Preloads were intensified with the incidence of occlusal forces. In the parallel implants, the force dissipation followed the long axis. The angled implant had a smaller quantity of fringes and the stresses were located mostly around the apical region of the lateral implants [*Cristiane, et al* (2004)].

A 3-D solid model of a human maxillary premolar was prepared and exported into a 3-D-finite element model (FEM) by *Ausiello, et al*, (2001) and a generic class II MOD cavity preparation and restoration was simulated in the FEM model by a proper choice of the mesh volumes. A validation procedure of the FEM model was executed based on a comparison of theoretical calculations and experimental data. Different rigidities were assigned to the adhesive system and restorative materials. Two different stress conditions were simulated: (a) stressesarising from the polymerization shrinkage and (b) stresses resulting from shrinkage stress in combination with vertical occlusal loading. Three different cases were analyzed: a sound tooth, a tooth with a class II MOD cavity, adhesively restored with a high (25GPa) and one with a low (12.5 GPa) elastic modulus composite. The cusp movements induced by polymerization stress and (over)-functional occlusal loading were evaluated. While cusp displacement was higher for the more rigid composites due to the prestressingfrom polymerization shrinkage, cusp movements turned out to be lower for the more flexible composites in case the restored tooth which was stressed by the occlusal loading.

This preliminary study by 3-D FEA on adhesively restored teeth with a class II MOD cavity indicated that Young's modulus values of the restorative materials play an essential role in the success of the restoration. Premature failure due to stresses arising from polymerization shrinkage and occlusal loading can be prevented by proper selection and combination of materials [*Ausiello, et al* (2001)].

Dentin bonding systems (DBS) have been developed in order to bond restorative materials (i.e. composite) to tooth tissues when function and integrity have to be re-established by *Santis, et al*, (2004). Adhesion to dentin results from the penetration of DBS into the demineralised substrate constituted by a conditioned collagen network. The long-term stability of a restored tooth is mainly affected by the seal of the restorative material on the dental structures.

Although leakage through the dentin–DBS interface has been widely reported, 3-D investigation technique and accurate nondestructive measurements of leakage as functions of mechanical cycling have never been provided. To address these issues, the properties of the material interface are analysed using micro-tensile static and dynamic tests, assisted by the finite element modeling and by the X-ray computed micro-tomography. The dual energy absorption technique, with the synchrotron beam light, has been developed to investigate, in a non-destructive manner, the effect of mechanical cycling on leakage of a silver nitrate staining solution at the dentin–DBS interface.

The effect of the pulpal roof on the stress distribution in the coronal dentin–DBS–composite interface has been investigated and the level at which the state of stress can be assumed to be uniform within acceptable limits has been defined. The tensile static and dynamic results suggest that the adhesive strength for the multi-step DBS resulted significantly higher than the other investigated DBS. Imaging results indicate that 3-D leakage occurs radially at the dentin–adhesive interface through the interface itself rather than through the unconditioned dentin bulk; moreover, the dynamic tensile loading allows a more diffuse staining penetration. [*Roberto, et al*, (2004)]

The objective of this study is to study the stresses and deformations in proximal dentine of human molar under simulated loading conditions. A finite element model of molar tooth was constructed based on a 3-D solid modeling using AutoCAD and exported to ANSYS FE program to calculate the stress deformation distributions on the molar tooth under loading condition with several angles 30°, 45°, 60° and 90°.

## 3 Finite element modeling for molar-tooth

The approach in this section is to model the molar-tooth by using the 3D finite element modelling capabilities of ANSYS. In this FE analysis, force applied with different angles are investigated. The objective of this study is to identify the stress and deformation of the molar-tooth under applied force with different angles which is activated to the model.

### 3.1 Molar-tooth finite element modelling and boundary conditions:

Two steps were used for modeling the molar tooth in this study firstly a 3-D solid modeling using AutoCAD and thin export the model to ANSYS for FE Analysis.

Figure 2 shows the molar-tooth modelling by ANSYS. A 3-dimensional structural mass element Solid is used for modelling the molar-tooth. The 3-D element SOLID92 with 6 degree of freedom is used for modelling the molar-tooth. The molar-tooth geometry was generated to 68851 elements as shown in Figure 2. The processing of the geometry and finite element mesh generation is provided by AutoCAD and ANSYS processing analysis to build the molar-tooth geometry.

The boundary conditions of the molar-tooth are:

Displacements in all three directions of the coordinate axes are zero at the roots of the tooth as shown in Figure 2:

$U_x = U_y = U_z = 0$.

Also rotations about all three coordinate axes are zero at the roots of the tooth as shown in Figure 2:

$Rot_x = Rot_y = Rot_z = 0$.

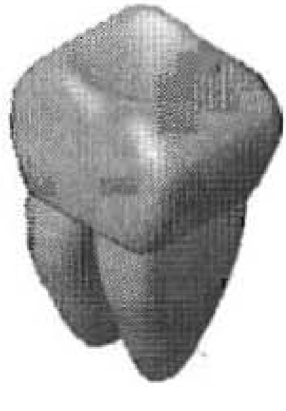

Figure 1: 3-D model

Figure 2: Boundary conditions for molar-tooth

### 3.2 Physical Properties

The following table 1 gives the assumed physical properties for the different materials:

Table 1: Material properties [*Genovese, et al (2004), and Lee, et al, (2002)*]

| Material | Yield modulus E (MPa) | Possion ratio's v |
|---|---|---|
| Enamel | 84100 | 0.20 |
| Dentine | 18600 | 0.31 |
| Pulp | 2 | 0.45 |

The molar-tooth contains three material which is Enamel, Dentine and pulp, as show figure 3 . The material used for the molar-tooth in this analysis is Dentine (see table 1).

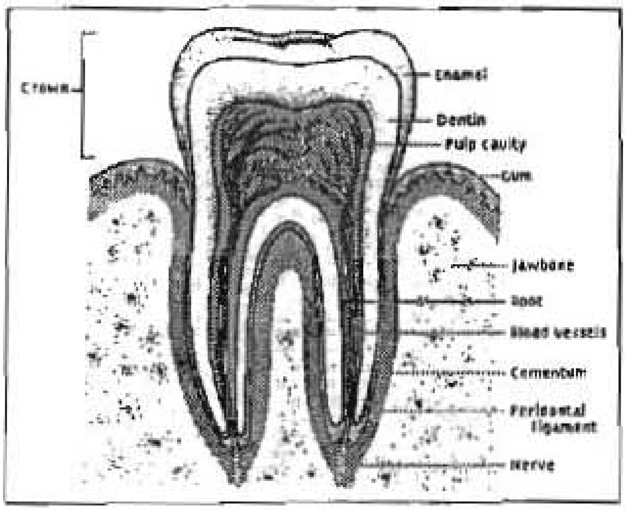


Figure 3: Structure of tooth [42]

## 4 Results and Discussion:

The results are presented for finite element analysis for molar-tooth with applied force with different angles

### 4.1 Variation of the applied force with different angles:

A static analysis is examined is used in several angles of the applied force, as detailed in sections 4-2-1-1 to 4-2-1-5:

#### 4.1.1 Applied force 1000 Newton with angle 30°

This force is applied with angle 30° to the molar-tooth. Figure 4 a,b,c,d shows the finite element results of the molar-tooth deformation and shearing stress profiles when applied force 1000 N with angle 30°. Both deformation and shearing stress profiles are indicated that the maximum deformation is 0.193521 mm and maximum shearing stress is 19783 MPa at the molar as shown figure 4 a,c, respectively. Figure 4 b,d also shows deformation and shearing stress along the molar-tooth and indicate that the place of maximum deformation and maximum shearing stress are left top end with $2.597\times10^{-1}$ mm and 4166 MPa, respectively.

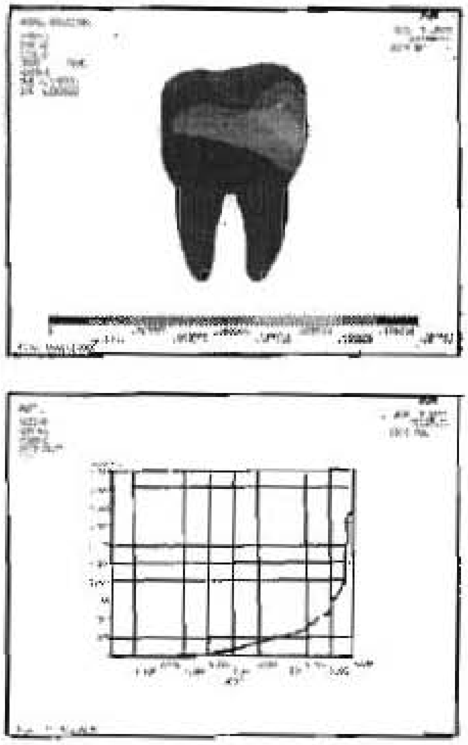

a) Distribution of deformation
b) Plot for change of deformation along molar

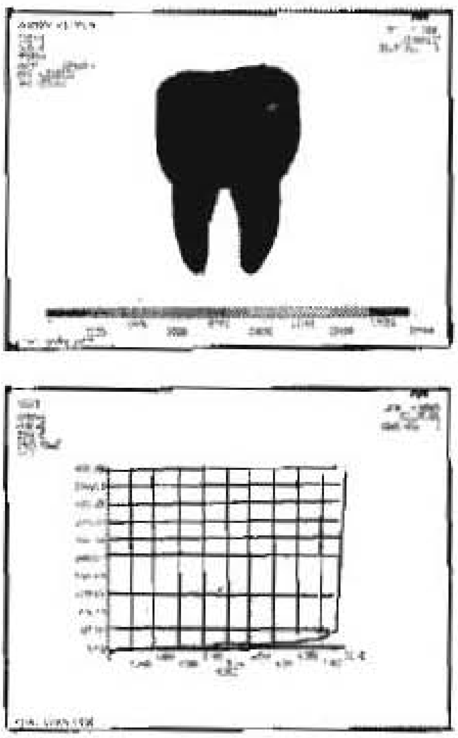

c) Distribution of shearing stress. d) Plot for change of shearing stress along molar

Figure 4 FEA of molar when applied force (1000 Newton) with angle (30°).

### 4.1.2 Applied force 1000 Newton with angle 45°

This force is applied with angle 45° to the molar-tooth. Figure 5 a,b,c,d shows the finite element results of the molar-tooth deformation and shearing stress profiles when applied force 1000 N with angle 45°. Both deformation and shearing stress profiles are indicated that the maximum deformation is 0.180631 mm and maximum shearing stress is 19533 MPa at the molar as shown figure 5 a,c, respectively. Figure 5 b,d also shows deformation and shearing stress along the molar-tooth and indicate that the place of maximum deformation and maximum shearing stress are left top end with $2.441\times10^{-1}$ mm and 3620 MPa, respectively.

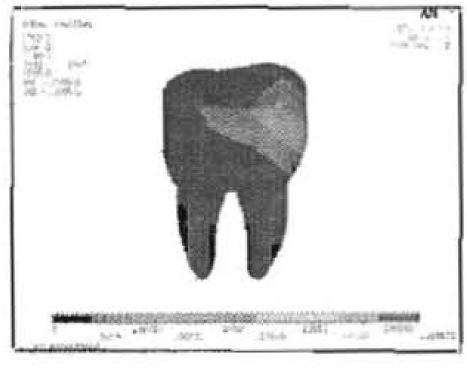

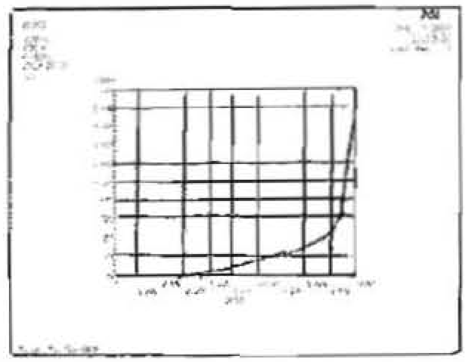

a) Distribution of deformation b) Plot for change of deformation along molar

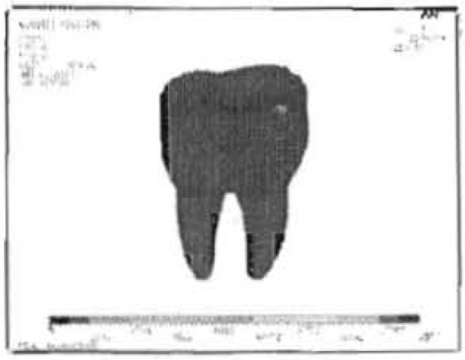

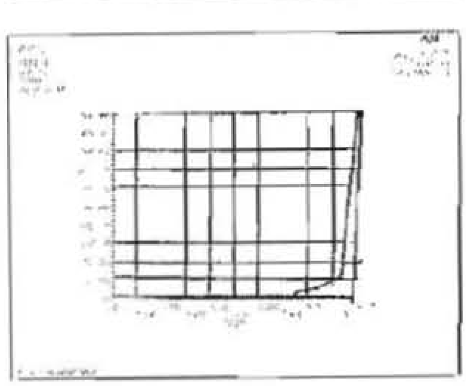

c) Distribution of shearing stress.
d) Plot for change of shearing stress along molar

Figure 5: FEA of molar when applied force (1000 Newton) with angle (45°)

### 4.1.3 Applied force 1000 Newton with angle 60°

This force is applied with angle 60° to the molar-tooth. Figure 6 a,b,c,d shows the finite element results of the molar-tooth deformation and shearing stress profiles when applied force 1000 N with angle 60°. Both deformation and shearing stress profiles are indicated that the maximum deformation is 0.159938 mm and maximum shearing stress is 19228 MPa at the molar as shown figure 6 a,c, respectively. Figure 6 b,d also shows deformation and shearing stress along the molar-tooth and indicate that the place of maximum deformation and maximum shearing stress are left top end with $2.244\times10^{-1}$ mm and 2913 MPa, respectively.

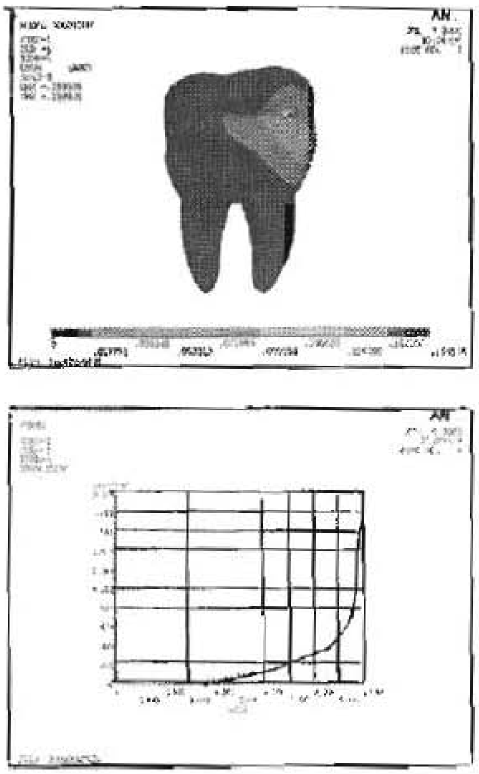

a) Distribution of deformation
b) Plot for change of deformation along molar

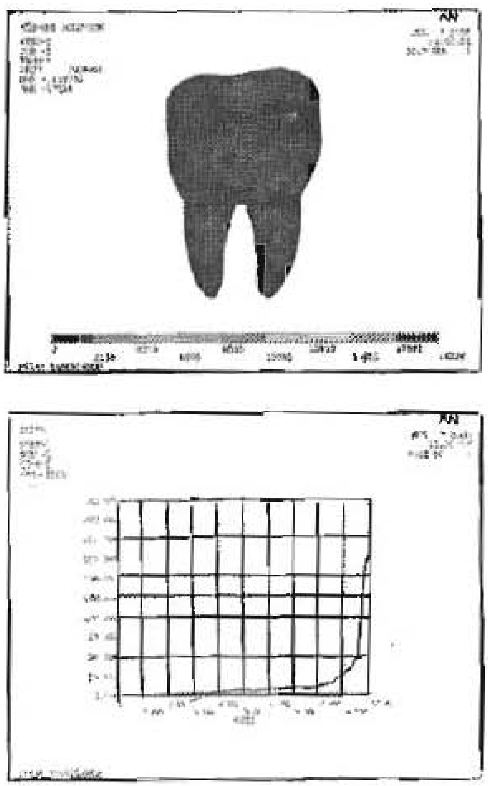

c) Distribution of shearing stress
d) Plot for change of shearing stress along molar

Figure 6 : FEA of molar when applied force (1000 Newton) with angle (60°).

#### 4.1.4 Applied force 1000 Newton with angle 90°

This force is applied with angle 90° to the molar-tooth. Figure 7 a,b,c,d shows the finite element results of the molar-tooth deformation and shearing stress profiles when applied force 1000 N with angle 90°. Both deformation and shearing stress profiles are indicated that the maximum deformation is 0.111344 mm and maximum shearing stress is 18761 MPa at the molar as shown figure 7 a,c, respectively. Figure 7 b,d also shows deformation and shearing stress along the molar-tooth and indicate that the place of maximum deformation and maximum shearing stress are left top end with $1.926\times10^{-1}$ mm and 1675 MPa, respectively.

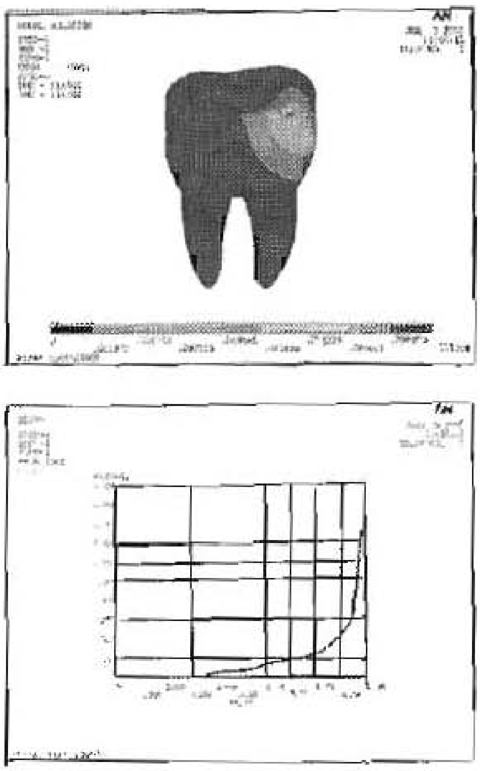

a) Distribution of deformation b) Plot for change of deformation along molar

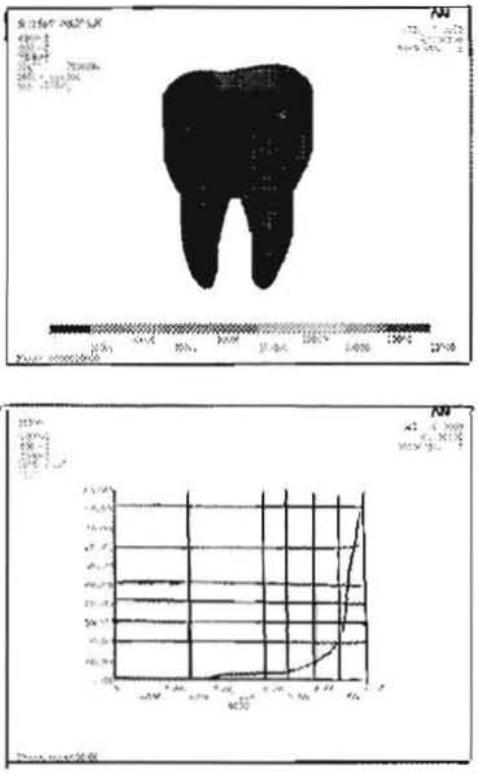

c) Distribution of shearing stress.
d) Plot for change of shearing stress along molar

Figure 7: FEA of molar when applied force (1000 Newton) with angle (90°).

#### 4.1.5 Comparison of effect of force with different angles:

The results show that deformation and stress is larger when the applied force with angle is 30° is more than other angles 45°, 60° and 90° as shown in figure 8 a,b.

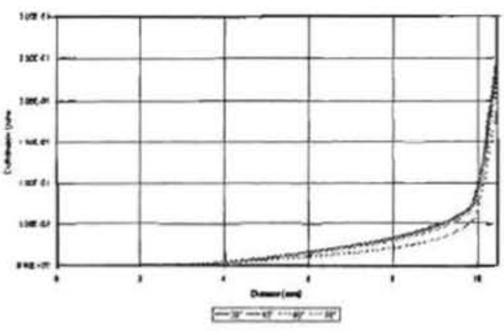

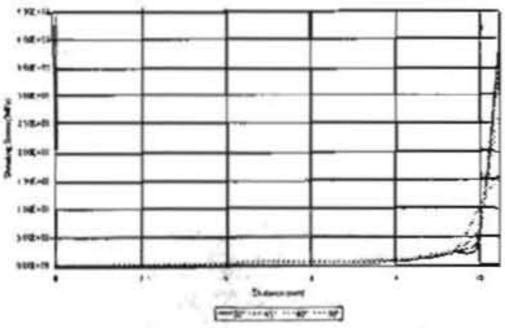

a) Deformation with different angles.
b) Stress with different angles.

Figure 8: Comparison of effect of applied force with different angles on molar

## 5 CONCLUSION AND RECOMMENDATIONS

### 5.1 Conclusion

The study presented in this research is a finite element analysis of the molar tooth to identify the stresses and deformations under loading condition with several angles 30°, 45°, 60°, 90°. The investigation were completed in this study with two steps , first one is a 3-D solid modeling for the molar tooth using AutoCAD and then export the solid model to the finite element identify package (ANSYS) to analyses the stresses and deformation using static analysis .
The test is used to indicate the stresses and deformation for the molar tooth under loading condition with several angles. The results indicate that the stresses and deformations increased with decreasing the directional angle of the applied load.

This study also is illustrate that is easier to model molar tooth structure by means of finite element package such as ANSYS and the analysis produce accurate and reliable results.

### 5.2 Recommendation for future work

There are several areas where more work is needed for analysis of molar-tooth. A few recommendations for future studies aimed at achieving this studies are listed below:

1- Variation of the load conditions for molar tooth using FE Analysis.

2- Study the effect of tooth cavities under several loading conditions on the stress distributions for the molar tooth.

3- Study and evaluate different filler materials in the cavities of the tooth and calculate this life's using FEA.

**References:**

A. Vila Verde, M.M.D.R., *Boundary conditions for 3D dynamic models of ablation of ceramics by pulsed mid-infrared lasers*. Applied Surface Science, 2005. 247: p. 354–361.

ANSYS release 8.0 documentation.

Arola D, Galles LA, Sarubin MF. *A comparison of the mechanical behavior of posterior teeth with amalgam and composite MOD restorations*. J Dent, 2001;29:63-73.

Beata Dejak, D., PhD, Andrzej M³otkowski, MEng, PhD, and Maciej Romanowicz, DDS, and PhD, *Finite element analysis of stresses in molars during clenching and mastication*. The Journal of Prosthetic Dentistry, 2003.

Bulent TOPBASI, M.G., Mustafa BAS, Cafer TURKMEN, *Two-dimensional Photoelastic Stress Analysis of Traumatized Incisor*. Braz Dent J, 2001. 12(2): p. 81-84.

Chris Ford , M.B.B., Xiao-Zhi Hu, Hong Zhao, *A numerical study of fracture modes in contact damage in porcelain/Pd-alloy bilayers*. Materials Science and Engineering, 2003: p. 202–206.

Cristiane Ueda, R.A.M., Cláudio Luiz Sendyk, Dalva Cruz Laganá, *Photoelastic analysis of stress distribution on parallel and angled implants after installation of fixed prostheses*. Braz Oral Res, 2004. 18(1): p. 45-52.

Darendeliler S, Darendeliler H, Kinoglu T. *Analysis of a central maxillary incisor using a three-dimensional finite element method*. J Oral Rehabil, 1992;19:371-383.

Dincer Bozkaya, M., a Sinan Muftu, MS, PhD,b and Ali Muftu, DMD, MS, PhDc, *Evaluation of load transfer characteristics of five different implants in compact bone at different load levels by finite elements analysis*. The Journal of Prosthetic Dentistry, 2004. 92: p. 523-30.

Eshleman JR, Janus CE, Jones CR. *Tooth preparation designs for resin-bonded fixed partial dentures related to enamel thickness*. J Prosthet Dent, 1988;60:18-22.

Goel VK, Khera SC, Singh K. *Clinical implications of the response of enamel and dentin to masticatory loads*. J Prosthet Dent, 1990;64:446-454.

Grippo JO. *Bioengineering seeds of contemplation: a private practitioner's perspective*. Dent Mater, 1996;12:198-202.

H. Fischer, M.W., M. Eck, A. Erdrich, R. Marx, *Finite element and experimental analyses of polymer-based dental bridges reinforced by ceramic bars*. Journal of Biomechanics, 2003: p. 289–294.

H.E. Lee, C.L.L., C.H. Wang , C.H. Cheng , C.H. Chang, *Stresses at the cervical lesion of maxillary premolar—a finite element investigation*. Journal of Dentistry, 2002: p. 283–290.

Hansen AR, Asmussen E, Christiansen NC. *In vivo fractures of endodontically treated teeth restored with amalgam*. Endod Dent Traumatol, 1990;6:49-55.

Jian-Ping Geng, B., MSD, Keson B. C. Tan, BDS (Hons), MSD, and Gui-Rong Liu, PhD, *Application of finite element analysis in implant dentistry: A review of the literature*. The Journal of Prosthetic Dentistry, 2001. 85: p. 585-98.

Jiwen Wang, L.L.S., *Rheological and extrusion behavior of dental porcelain slurries for rapid prototyping applications*. Materials Science and Engineering, 2005: p. 314–321.

K. Genovese , L.L., C. Pappalettere, *Finite element analysis of a new customized composite post system for endodontically treated teeth*. Journal of Biomechanics, 2004.

Kaewsuriyathumrong C, Soma K. *Stress of tooth and PDL structure created by bite force*. Bull Tokyo Med Dent Univ, 1993;40:217-232.

M. Sevimay, D., PhD, F. Turhan, DDS, M. A. Kilicxarslan, PhD, and G. Eskitascioglu, DDS, PhD, *Three-dimensional finite element analysis of the effect of different bone quality on stress distribution in an implant-supported crown*. THE JOURNAL OF PROSTHETIC DENTISTRY, 2005. 93: p. 227-34.

Manjing Deng , J.S., Anthony J. Smith , Yan Jin, *Effects of transforming growth factor b1 (TGFb-1) and dentin non-collagenous proteins (DNCP) on human embryonic ectomesenchymal cells in a three-dimensional culture system*. Archives of Oral Biology, 2005.

Microsoft Encarta Deluxe 2002.

Mondelli J, Steagall L, Ishikiriama A, Navarro M, Soares FB. *Fracture strength of human teeth with cavity preparations*. J Prosthet Dent, 1980;43:419-422.

Morin DL, Cross M, Voller VR, Douglas WH, DeLong R. *Biophysical stress analysis of restored teeth: modelling and analysis*. Dent Mater, 1988;4:77-84.

Niek De Jager, P.P., Albert J. Feilzer, *Finite element analysis model to simulate the behavior of luting cements during setting*. Dental Materials, 2004: p. 1–8.

Niek De Jager, P.P., Albert J. Feilzer, *The apparent increase of the Young's modulus in thin cement layers*. Dental Materials, 2003. 20: p. 457–462.

Niek De Jager, P.P., Albert J. Feilzer, *The influence of design parameters on the FEA-determined stress distribution in CAD–CAM produced all-ceramic dental crowns*. Dental Materials, 2004. 21: p. 242–251.

Omer Lutfi Koca, D., PhD, Gurcan Eskitascioglu, DDS, PhD, and Aslihan Usumez, DDS, PhD, *Three-dimensional finite-element analysis of functional stresses in different bone locations produced by implants placed in the maxillary posterior region of the sinus floor*. THE JOURNAL OF PROSTHETIC DENTISTRY, 2005. 93: p. 38-44.

P. Ausiello, A.A., C.L. Davidson, S. Rengo, *3D-finite element analyses of cusp movements in a human upper premolar, restored with adhesive resin-based composites*. Journal of Biomechanics, 2001: p. 1269–1277.

Paolo M. Cattaneo, M., Michel Dalstra, PhD, and Birte Melsen, DDS, dr odont, *The transfer of occlusal forces through the maxillary molars: A finite element study*. American Journal of Orthodontics and Dentofacial Orthopedics, 2003. 123: p. 367-73.

Paul H. DeHoff , K.J.A., Nils Götzen, *Viscoelastic finite element analysis of an all-ceramic fixed partial denture*. Journal of Biomechanics, 2004.

Peter D. Jeon, M., DDS, Patrick K. Turley, DDS, MSD, MEd, and Kang Ting, DMD, DMSc, *Three-dimensional finite element analysis of stress in the periodontal ligament of the maxillary first molar with simulated bone loss*. American Journal of Orthodontics and Dentofacial Orthopedics, 2001. 119: p. 498-504.

Pietro Ausiello , A.A., Carel. L . Davidson, *Effect of adhesive layer properties on stress distribution in composite restorations –a 3D finite element analysis*. Dental Materials, 2001: p. 295-303.

Pietro Ausiello , S.R., Carel L. Davidson, David C. Watts, *Stress* *distributions in adhesively cemented ceramic and resin-composite Class II inlay restorations: a 3D-FEA study.* Dental Materials, 2004. 20: p. 862–872.

Powers, R.G.C.J.M., *Restorative Dental Materials.* 11 ed. 1960, USA: Mosby.

R.C. Atwooda, P.D.L., , R.V. Curtis, *Modeling the surface contamination of dental titanium investment castings.* Dental Materials, 2005. 21: p. 178–186.

Ralf J. Radlanski, H.R., *Explainable and critical periods during human dental morphogenesis and their control.* Archives of Oral Biology, 2004. 50: p. 199—203.

Reeh ES, Messer HH, Douglas WH. *Reduction in tooth stiffness as a result of endodontic and restorative procedures.* J Endod, 1989;15:512-516.

Roberto De Santis , F.M., Davide Prisco, Sandro Rengo, and L.N. Luigi Ambrosio, *A 3D analysis of mechanically stressed dentin–adhesive–composite interfaces using X-ray micro-CT.* Biomaterials, 2004: p. 257–270.

Sakaguchi RL, Brust EW, Cross M, DeLong R, Douglas WH. *Independent movement of cusps during occlusal loading.* Dent Mater, 1991;7:186-190.

Shosei Eguchi, G.C.T., Lindsay C. Richards, Toby Hughes, Kazutaka Kasai, *Genetic contribution to dental arch size variation in Australian twins.* Archives of Oral Biology, 2004. 49: p. 1015—1024.

Thresher RW, Saito GE. *The stress analysis of human teeth.* J Biomech, 1973;6:443-449.

Tidmarsh BG. *Restoration of endodontically treated posterior teeth.* J Endo, 1976;2:374-375.

V. Pattijn, C.V.L., G. Van der Perrea, I. Naerte, J. *Vander Sloten, The resonance frequencies and mode shapes of dental implants: Rigid body behaviour versus bending behaviour.* A numerical approach. Journal of Biomechanics, 2005.